Open Access

Check for updates

Research Article

Journal of Veterinary and Animal Sciences
ISSN (Print): 0971-0701, (Online): 2582-0605
https://doi.org/10.51966/jvas.2026.57.1.46-54

Preparation and characterisation of decellularised porcine tunica vaginalis-based hydrogels for wound healing application

Pooja Kailas[1], B. Dhanush Krishna[2*], Hamza Palekkodan[1], V.N Vasudevan[3], R.Rajasekhar[4], M. Pradeep[1], Ajith Jacob George[5] and P. Kushwanth Sai Kumar[4]

[1]Department of Veterinary Pathology, [4]Department of Veterinary Microbiology, College of Veterinary and Animal Sciences, Pookode, Wayanad-673 576, [2]Department of Veterinary Pathology, [3]Department of Livestock Products Technology, College of Veterinary and Animal Sciences, Mannuthy, Thrissur, Kerala Veterinary and Animal Sciences University, Pookode, Wayanad, Kerala

Citation: Pooja, K., Dhanush, K.B., Hamza, P., Vasudevan, V.N., Rajasekhar, R., Predeep, M., George, A.J. & Kumar, P.K.S. (2026). Preparation and characterisation of decellularised porcine tunica vaginalis-based hydrogels for wound healing application. *Journal of Veterinary and Animal Sciences* 57 (1), 46-54
https://doi.org/10.51966/jvas.2026.57.1.46-54

Received: 09.09.2025 Accepted: 05.11.2025 Published: 31.03.2026

Abstract

Hydrogels, with extracellular matrix (ECM) like properties, support tissue regeneration by maintaining moisture and oxygen diffusion. In this study, a hydrogel was developed from decellularised porcine tunica vaginalis (DPTV) blended with carboxymethyl cellulose (CMC) and crosslinked using ferric chloride for wound healing applications. The DPTV was prepared by subjecting porcine tunica vaginalis to a sequential decellularisation with enzymatic and detergent treatments, followed by homogenisation, lyophilisation, and blending with CMC to produce pre-gel suspensions. Four hydrogel formulations (HG50, HG60, HG70, and HG80) with varying DPTV to CMC ratios were prepared and further evaluated for physical properties such as colour, texture, transparency, consistency, gel fraction, and water absorption per cent and topography. Results revealed that HG60 exhibited the most balanced characteristics with an adequate gel fraction (88.7%) ensuring mechanical stability, a favourable water absorption percent (76.4%) supporting moisture retention and a spongy architecture by scanning electron microscopy for water absorption. Thus, we developed a formulation that exhibited good water-holding capacity which results in better absorption of exudates and structural stability for wound healing applications. The findings warrant evaluation in pre-clinical models to test the efficacy of DPTV–CMC hydrogels as bioactive wound dressing for accelerating tissue repair and regeneration for potential wound healing application.

Keywords: *Hydrogel, carboxy methyl cellulose, extra cellular matrix, biocompatibility*

Skin wounds are among the most common conditions encountered in both human and veterinary medicine. Wound healing is a highly coordinated and dynamic biological process that progresses through three overlapping phases: inflammation, proliferation, and remodelling, during which damaged tissue is repaired and wound closure is achieved (Christanto et al., 2025). When this progression is disrupted, chronic wounds may develop, often complicated by persistent infections, poor circulation, systemic conditions such as diabetes, species-specific challenges, patient compliance issues, and financial constraints that collectively delay recovery (Guo et al., 2022). Therefore, there is an

Corresponding author: dhanush@kvasu.ac.in, Ph. 9497891394

increasing demand for effective wound healing strategies, with natural biomaterials like porcine tunica vaginalis emerging as promising ECM-mimicking scaffolds due to their biocompatibility and structural similarity to native tissue.

Since the 19th century, plasters, bandages, gauzes, and topical ointments have been the most widely used wound dressings because they are inexpensive and easy to apply (Rezvani et al., 2023). Although these dressings protect the wound from infection and absorb exudate, they fail to regulate moisture effectively, often causing excessive dryness or dampness that impairs optimal healing (Rezvani et al., 2019). Consequently, research has increasingly focused on designing innovative wound-healing materials.

Due to ideal cellular microenvironment mimicking and good biocompatibility, tissue -derived ECM is a highly promising biomaterial for tissue engineering applications (Balakrishnan et al., 2018; Guan et al., 2022). Therefore, there is an increasing demand for effective wound healing strategies, with natural biomaterials like porcine tunica vaginalis emerging as a promising ECM-mimicking scaffold due to their biocompatibility and structural similarity with native tissue (Adly et al., 2024). Hydrogels are one such dressing material which possess a three-dimensional polymer network capable of absorbing significant amounts of water while maintaining structural integrity, making them promising for wound healing applications (Rao et al., 2021). Their high water content mimics the ECM, providing a moist environment that minimises scarring, soothes pain, and prevents tissue adhesion (Koehler et al., 2018; Kumar and Kaur, 2020). Additionally, their porous structure promotes oxygen diffusion and tissue regeneration while their swelling capacity enhances exudate absorption (Stubbe et al., 2019; Singh and Kumar, 2020).

Hydrogels derived from the ECM whether sourced from decellularised tissues or engineered recombinant proteins improve wound repair by mimicking natural tissue structure, facilitating cell migration, blood vessel formation, and regenerative growth (Wolf et al., 2012). Earlier research on DPTV has demonstrated its potential as a biocompatible scaffold, making it suitable for tissue engineering and regenerative medicine applications (Arathy et al., 2023; Abin et al., 2025). With their ability to closely mimic native tissue and enhance regeneration, extracellular matrix hydrogels hold immense potential as next-generation wound dressings, paving the way for advanced, bioengineered healing solutions. With this background, the present study was designed to prepare and characterise an ECM-based hydrogel derived from DPTV, which can exhibit an optimal balance of gel fraction, water absorption percent, and structural stability for effective wound healing applications.

Materials and methods

Preparation of decellularised porcine tunica vaginalis

The porcine tunica vaginalis was manually defatted using a scrapper, followed by chemical defatting in a chloroform-methanol mixture (2:1 v/v) for 12 hours. After defatting, the samples were rinsed with deionised water in an incubator shaker (120 rpm, 1 hour). An initial detergent wash with 1% Triton-X-100 was performed for 30 minutes at room temperature to eliminate residual solvents. Next, the samples were treated with 0.05% Trypsin and 0.02% EDTA for 4 hours at room temperature in an incubator shaker (150 rpm). Following a deionised water rinse (150 rpm, 1 hour), the tissues were exposed to 1% sodium deoxycholate (SDC) for 4 hours at 150 rpm. Finally, the samples were incubated in 1 kU/mL DNase for 6 hours at room temperature, washed with 1X PBS, and stored at 4°C until further processing (Arathy et al., 2023).

The decellularised tunica vaginalis was fixed at 10 percent neutral buffer formalin (NBF). The fixed tissue was then washed, dehydrated, and embedded in paraffin. Sections were made in 5 µm thickness, stained with H&E, Masson's Trichrome and Picrosirius red staining and subjected to microscopic examination (Luna, 1968).

Preparation of hydrogel

Following decellularisation, the tissue was homogenised into a paste, spread onto a petri dish, and lyophilised for 20 hours. The freeze-dried tissue was then ground into fine strands using a mixer. The ground tissue was subsequently cut into smaller fragments with scissors, reground, and stored in a desiccator until further use.

Using distilled water, a 5% w/v suspension of powdered DPTV and carboxymethyl cellulose (CMC) 3% w/v suspension was made in distilled water at the same time. For four hours, each suspension was agitated independently with magnetic stirrers to guarantee even dispersion. In order to create pregel suspension, the

Table 1. List of DPTV-CMC hydrogel formulations

Sl. No.	Hydrogel formulations	Proportion of the DPTV suspension (%)	The proportion of CMC solution (%)
1	Gel50	50	50
2	Gel60	60	40
3	Gel70	70	30
4	Gel80	80	20

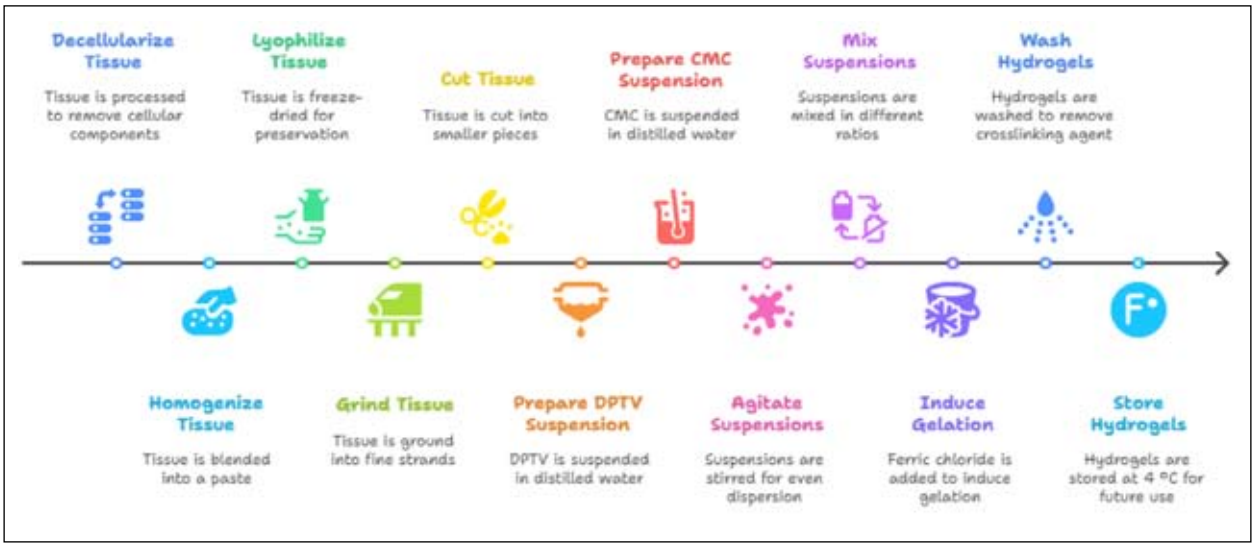

Fig. 1. Schematic diagram showing the preparation steps of extra cellular matrix – derived hydrogel (The picture was created using the Napkin AI application)

suspensions were then mixed in four different ratios, as shown in Table 1. Each pregel was added to an equivalent amount of a 7 mM ferric chloride solution to induce gelation and promote crosslinking. Gel50, Gel60, Gel70, and Gel80 were the names given to the resultant hydrogels, which corresponded to the percent of DPTV in each formulation (Pratheesh et al., 2025). After two minutes of crosslinking with ferric chloride, the hydrogels were collected and thoroughly washed with sterile distilled water to remove any residual crosslinking agent. The final hydrogels were transferred into sterile vials, sealed with parafilm, and stored at 4 °C until further characterisation.

Physical characterisation of hydrogel

a. Gross appearance

The gross appearance of hydrogel including the colour, consistency, transparency and texture were assessed and are represented in Table 2.

b. Gel fraction percent

Hydrogel samples (2 g) were dried at 50 °C for 6 hours to determine their initial dry weight (W_0). Samples were then placed in Petri dishes containing 10 mL of distilled water and allowed to soak for 24 hours to ensure the removal of soluble fractions. After soaking, the samples were carefully removed and re-dried at 50 °C to obtain the final dry weight (W_e). The gel fraction per cent was calculated using the following equation:

$$\text{Gel fraction } \% = \left(\frac{We}{Wo}\right) \times 100$$

Where W_o and W_e are the weights of hydrogel samples dried for 6 h at 50°C before and after soaking, respectively (Hwang et al., 2010)

c. Water absorption percent (WAP)

The hydrogel samples were immersed in distilled water at fixed time intervals while maintaining a constant temperature of 37 °C. At each interval, excess surface water was gently blotted using filter paper, and the swollen weight of the hydrogels was recorded. This process was continued for almost an hour until the samples showed no further increase in weight, indicating equilibrium swelling.

$$\text{Water absorption } \% = \left(\frac{Ws-Wd}{Ws}\right) \times 100$$

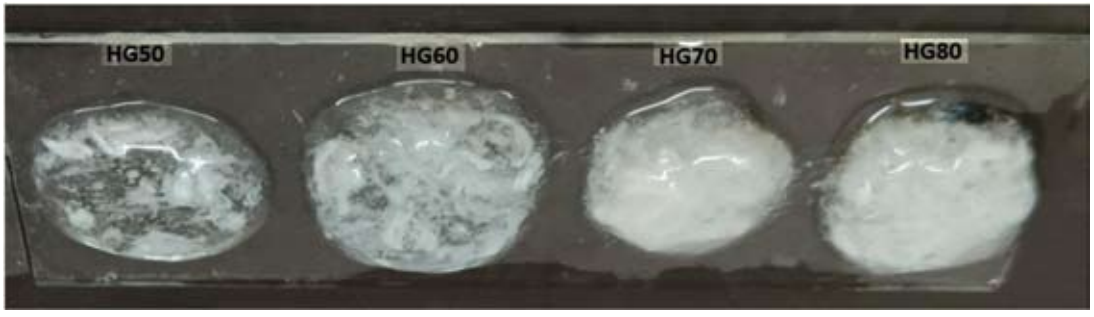

Fig. 2. Gross appearance of different formulations of PTV-CMC (HG50: slightly translucent and smooth, gelatinous; HG60: slightly opaque and firm; HG60: uniform, soft gel; HG80: dense and compact.

Here, W_s is the mass of the swollen gel at time t and W_d is the mass of the dry gel at time 0 (Yoo et al., 2008).

d. Scanning electron microscopy

The lyophilised samples, after being air-dried, were fixed onto metal stubs using double-sided carbon adhesive tape. Subsequently, they were sputter-coated with a thin layer of gold and examined under a scanning electron microscope (Jeol JSM 6390LA) operated at an accelerating voltage of 20 kV, where electron micrographs were captured (Pratheesh et al., 2025).

Results and discussion

Efficiency of decellularisation

The decellularised tunica vaginalis prepared by combined decellularisation protocol using combination of Trypsin-EDTA-Triton X-100 SDC-DNase appeared as a thin, sheet-like membrane with a uniform pale white coloration (Fig. 3B). The surface was smooth with faint fibrous striations, reflecting the preserved collagenous architecture of the extracellular matrix. The tissue maintained its native shape and mechanical integrity, exhibiting flexibility yet notable tensile strength without signs of tearing or brittleness. The absence of discoloration or visible cellular debris confirmed the effectiveness and cleanliness of the decellularisation process.

Histological evaluation

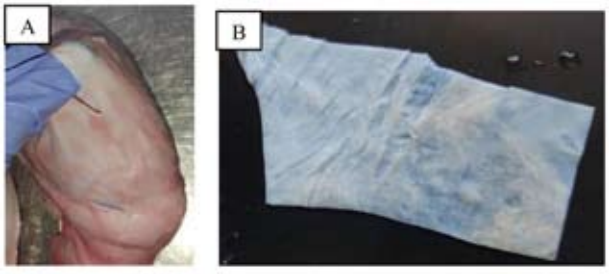

Fig. 3. A. Porcine tunica vaginalis tissue, **B**. Decellularised porcine tunica vaginalis derived extracellular matrix

Histological assessment of the DPTV scaffold using haematoxylin and eosin (H&E) staining confirmed the successful removal of cellular components. The tissue sections demonstrated a complete absence of nuclei and nuclear remnants that would typically appear blue with haematoxylin similar to the findings of Nath et al. (2025). The ECM was well-preserved, with eosinophilic staining revealing densely packed, wavy collagen fibres in varying shades of pink (Fig. 4). In DPTV, Masson's trichrome staining revealed collagen fibres as blue (Fig. 4B), while Picrosirius red staining highlighted them in bright red to orange shades (Fig. 4C). The organised collagen architecture together with the absence of cellular material, validated the efficiency of the decellularisation process, and underscored the scaffold's potential as a biocompatible framework for tissue regeneration (Nath et al., 2025).

Homogenisation of the decellularised porcine tunica vaginalis

The homogenised porcine tunica vaginalis tissue appeared as an off-white to pale, fibrous mass with irregular, thread-like structures. It exhibited a dense, tough, and resilient texture, characterised by tightly interwoven fibres that were difficult to break apart manually. The material displayed a web-like morphology with an uneven,

Fig. 5. Homogenised porcine tunica vaginalis

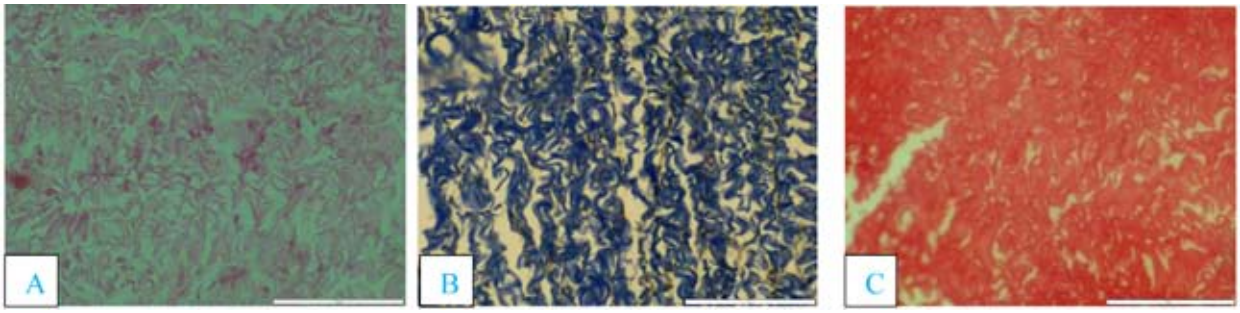

Fig. 4. Histomorphology of DPTV; **A.** H and E stain with eosinophilic matrix with absence of nuclear remnants (H&E x 400); **B.** Dark blue collagen fragments under Masson's trichrome stain (MTC x 400); **C.** Bright red collagen bundles under picrosirius red stain (PSR x 400).

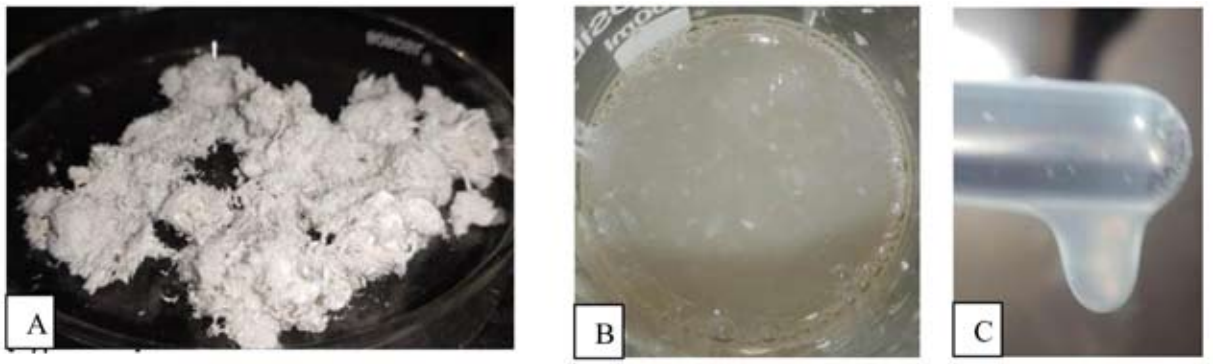

Fig. 6 **A**-Powdered porcine tunica vaginalis; **B**- Suspension of CMC and powdered porcine tunica vaginalis; **C**- Dripping consistency of the solution

entangled arrangement across the Petri dish (Fig. 5). The absence of discoloration or debris suggested that the tissue was processed under clean and controlled conditions, preserving its structural integrity.

Preparation of powdered decellularised porcine tunica vaginalis to hydrogel

The powdered decellularised porcine tunica vaginalis tissue appeared as a pale, fibrous mass with a dry, fluffy consistency and a white coloration, indicating successful decellularisation and lyophilisation (Fig. 6.A). Upon blending with a 3% (w/v) carboxymethylcellulose (CMC) solution, a uniform semi-viscous mixture was obtained, forming a smooth, opaque suspension with no visible clumps (Fig. 6.B). The final formulation exhibited a gel-like consistency with moderate viscosity and cohesive flow characteristics, as evidenced by the stretching and dripping pattern observed when lifted (Fig. 6.C). This consistency suggests good interaction between the structural matrix of the decellularised scaffold and the polymeric network of CMC may be suitable for potential wound dressing applications.

Following cross-linking with ferric chloride, the hydrogel exhibited a firm, self-supporting, and gelatinous consistency, indicating successful gelation (Fig. 7).

Fig. 7. Porcine tunica vaginalis was crosslinked using ferric chloride for preparing hydrogel

Characterisation of hydrogel

Physical characteristics of the hydrogel

a. Gross appearance

The gross appearance of the hydrogels, such as colour, texture, transparency, and consistency, varied significantly depending on the ratio of DPTV to carboxymethylcellulose (CMC) (Table 2). These characteristics were essential for assessing the suitability of hydrogel for biomedical uses, especially in wound healing.

b. Colour and transparency

The colour of the hydrogels changed from pale white (HG50) to milky white (HG80) as the per cent of DPTV increased, suggesting a greater concentration of tissue-derived components. A progressive reduction in transparency was also associated with this colour shift. Whereas HG70 and HG80 were entirely opaque, HG50 and HG60 seemed to be slightly to moderately translucent. Increased protein concentration and matrix density may be the cause of reduced transparency at higher DPTV content (Pratheesh et al., 2025).

c. Texture and Consistency

All formulations demonstrated smooth textures; however, their firmness varied significantly. HG50 presented a soft and moderately firm texture, while HG60 formed a more gelatinous and cohesive structure. As the DPTV ratio increased further in HG70 and HG80, the hydrogels became progressively firmer and more compact. HG80, with the highest DPTV content, exhibited the most rigid and stable structure**.**

d. Gel fraction percent

The gel fraction analysis over 20 minutes revealed a gradual decrease in all formulations as shown in (Fig. 8) due to the leaching of loosely bound polymers. The gel fraction represents the crosslinking density of the

Table 2. Gross and physical appearance of the formulations

Hydrogel Code	Blending Ratio (DPTV:CMC)	Colour	Texture	Transparency	Consistency
HG50	50:50	Pale white	Smooth and soft	Slightly translucent	Moderately firm
HG60	60:40	Off-white	Smooth, gelatinous	Translucent	Firm and cohesive
HG70	70:30	White	Uniform, soft gel	Slightly opaque	Firmer than HG60
HG80	80:20	Milky white	Dense and compact	Opaque	Most rigid and stable

hydrogel, with higher values indicating a more stable and insoluble network resistant to dissolution (Yu et al., 2022). Gel50 showed the highest gel fraction (78.4%%), while Gel80 had the lowest (59.9%). A reduced gel fraction may weaken the mechanical strength and structural stability of the hydrogel, potentially limiting its effectiveness in supporting cell migration and tissue regeneration (Lei et al., 2017). A high gel fraction improved the structural stability, mechanical strength, and long-term durability of hydrogel, which was crucial for preserving its shape and functionality, particularly in tissue engineering and wound dressing applications (Demeter et al., 2023). An excessively high gel fraction could restrict swelling, thereby reducing the capacity of hydrogel for water retention and controlled drug release (Asy et al., 2022).

e. Water Absorption Percent (WAP)

The WAP analysis over 60 minutes revealed a gradual decrease in all formulations as shown in Table 13 and Fig. 2 due to the leaching of loosely bound polymers. HG80 showed the highest WAP (89.8%), while HG50 had the lowest (81.1%). The water holding capacity reflects the ability to retain moisture, where greater values denote improved hydration and swelling, essential for sustaining cellular activity and tissue repair (Martinez et al., 2022).

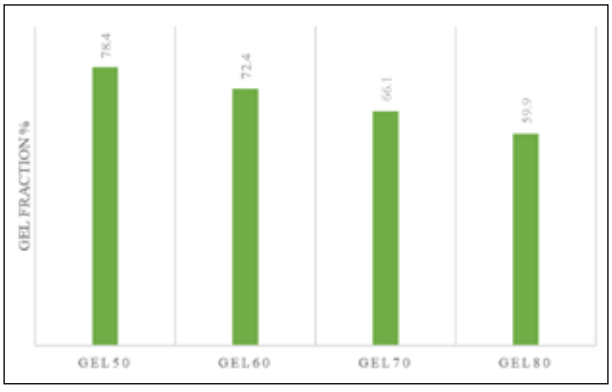

Fig. 8. A bar diagram showing gel fraction per cent of the hydrogel formulations

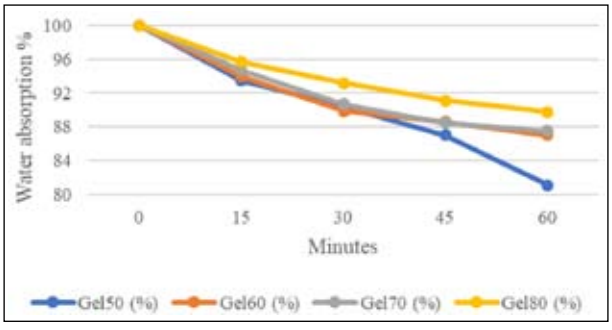

Fig. 9. A line graph showing water absorption percent of the hydrogel formulations

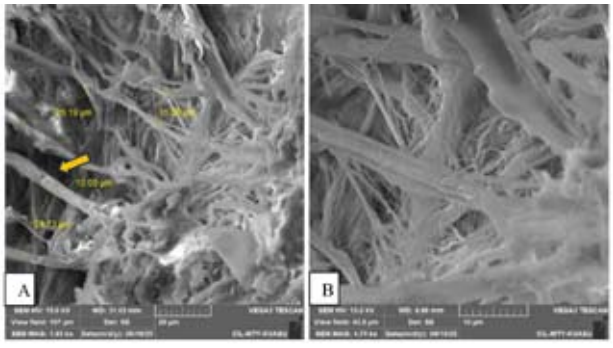

Fig. 10. Scanning electron microscopy image of hydrogel **A**. Porous structure visible in between the fibres (arrow) (SEMx600) **B**. Mesh-like architecture of hydrogel (SEMx300)

f. Scanning electron microscopy

The SEM image revealed a rough, mesh-like morphology of the hydrogel with distinct macro porous spaces between the fibres, consistent with the findings of Yasin *et al*. (2024), who reported that greater surface roughness and well-optimised pore size enhance cell adhesion, water absorption, and regulated release of therapeutic agents, ultimately promoting faster wound healing (Fig. 10A and 10B).

Hydrogels are among the most promising wound dressing materials owing to their excellent water-retention capacity, attributed to their cross-linked three-dimensional network structure (Rao et al., 2021). Hydrogels can be fabricated through various crosslinking mechanisms, which may involve either reversible or irreversible interactions (Johnson et al., 2020). In the present study, the DPTV hydrogel was developed *via* ionic physical crosslinking. Carboxymethyl cellulose (CMC) is a negatively charged polysaccharide owing to the presence of $–COO^-$ groups, interacts with ferric ions derived from the dissociation of $FeCl_3$ in aqueous medium. The trivalent Fe^{3+} ions serve as bridging agents between the carboxylate groups of CMC, thereby establishing ionic crosslinks (Liu et al., 2023). Such interactions typically enhance the structural integrity of the hydrogel, contributing to improved thermal stability and swelling behaviour (Kumar et al., 2020). The extent of crosslinking and the resulting physicochemical

properties are strongly influenced by Fe^{3+} concentration, the degree of CMC substitution, and mixing conditions (Zhang et al., 2022). Extracellular matrix (ECM) scaffolds are typically generated through physical, chemical, or enzymatic decellularisation techniques to ensure the complete removal of cellular components while maintaining the native architectural integrity (McInnes et al., 2022). In this study, decellularisation of the scaffold was achieved using the combined protocol proposed by Arathy *et al*. (2023), and the processed scaffold was subsequently converted into an ECM hydrogel with the incorporation of CMC and $FeCl_3$. After preparation of the ECM hydrogel, its physicochemical characteristics such as gel fraction, WAP, and surface topography were analysed to assess their effects on stability, hydration efficiency, and overall applicability in wound healing. Among the tested formulations, HG50 exhibited the highest gel fraction (78.4%), indicating strong crosslinking and mechanical robustness (Greene et al., 2023). However, a low WAP (81.1%) of hydrogel reflects diminished moisture retention, which may substantially compromise its functionality in wound healing applications (Yasin et al., 2024). Conversely, HG80 demonstrated the highest WAP (89.8%), supporting a favourable moist environment, but its lower gel fraction (59.9%) implied weaker structural integrity, potentially leading to premature degradation under physiological conditions (Yang, 2012). HG60 emerged as the most balanced formulation, with a gel fraction of 72.4% and an WAP of 87%. This intermediate crosslinking density provided sufficient mechanical stability while retaining optimal hydration, a key requirement for effective wound healing (Pratheesh et al., 2025). The SEM image revealed a rough, mesh-like morphology of the hydrogel with distinct macro porous spaces between the fibres, consistent with the findings of Yasin et al. (2024), who reported that greater surface roughness and well-optimised pore size enhance cell adhesion, water absorption, and regulated release of therapeutic agents, ultimately promoting faster wound healing. Macroscopically, HG60 exhibited a cohesive yet flexible consistency, ensuring uniform wound coverage without being overly rigid or fragile. Consequently, HG60 formulation was selected as the most suitable candidate for wound healing applications, combining structural durability with the necessary hydrophilic properties to facilitate tissue repair.

Therefore, HG60 was chosen as the optimal candidate for wound healing applications, as it effectively integrates mechanical stability with hydrophilic characteristics that support tissue regeneration. Considering the collective evaluation of gel fraction, WAP, mechanical texture, and SEM findings, HG60 was concluded to be the most suitable formulation, and hence was finalised for the preparation of the ECM hydrogel. This study highlights the need of potential of natural biomaterial-based hydrogels that could broaden their applications of effective wound repair strategies in clinical practice.

Conclusion

To address the challenges of wound healing, we developed a biocompatible hydrogel composed of DPTV and CMC, with favourable physicochemical properties for wound repair. By optimising polymer content and concentration of cross-linking agent, the hydrogel displayed adjustable gel fraction, WAP and a fibrous interconnected microarchitecture. Among the formulations, HG60 demonstrated the most favourable balance between mechanical integrity and hydration capacity, supported by its porous microstructure and pliable consistency. These findings highlight HG60 as a promising bioactive wound dressing that mimics native ECM and can foster an optimal environment for tissue repair and regeneration.

Acknowledgements

The financial support provided by Kerala Veterinary and Animal Sciences University is greatly acknowledged.

Conflict of interest

The authors declare that they have no conflict of interest.

References

Abin, J. P., Dhanush, K. B., George, A. J., Pradeep, M., Vasudevan, V. N., & Pooja, K. (2025). Comparative evaluation of mechanical properties of decellularised non-cross-linked and cross-linked porcine tunica vaginalis. *Journal of Veterinary and Animal Sciences, 56*, 332–337.

Adly, H. A., El-Okby, A. W. Y., Yehya, A. A., El-Shamy, A. A., Galhom, R. A., Hashem, M. A., & Ahmed, M. F. (2024). Circumferential esophageal reconstruction using a tissue-engineered decellularized tunica vaginalis graft in a rabbit model. *Journal of Pediatric Surgery*.

Arathy, P. S., Balakrishnan-Nair, D. K., Vasudevan, V. N., Sajitha, I. S., Joseph, J., Saifudeen, S. M., & Prasanna, K.S. (2023). Evaluation of decellularisation protocols for developing extracellular matrix-based porcine tunica vaginalis scaffolds for tissue engineering applications. *Exploratory Animal and Medical Research, 13*, 22–30.

Asy-Syifa, N., Waresindo, W. X., Edikresnha, D., Suciati, T., & Khairurrijal, K. (2022). The study of the swelling degree of the PVA hydrogel with varying concentrations of PVA. *Journal of Physics: Conference Series, 2243*, 012053.

Balakrishnan-Nair, D. K., Nair, N. D., Venugopal, S. K., Das, V. N., George, S., Abraham, M. J., & Anilkumar, T. V.

(2018). An immunopathological evaluation of the porcine cholecyst matrix as a muscle repair graft in a male rat abdominal wall defect model. *Toxicologic Pathology, 46*, 169–183.

Christanto, A., Cilmiaty, R., Setiamika, M., Yudhani, R. D., Dirgahayu, P., Pamungkasari, E. P., & Nurwati, I. (2025). The role of interleukin 1β, fibroblast growth factor, fibroblasts, keratinocytes, granulation tissue and collagen density in the wound healing phase. *Biocaster: Jurnal Kajian Biologi, 5*, 108–118.

Demeter, M., Scărișoreanu, A., & Călina, I. (2023). State of the art of hydrogel wound dressings developed by ionizing radiation. *Gels, 9*(1), 55.

Greene, C., Beaman, H. T., Stinfort, D., Ramezani, M., & Monroe, M. B. B. (2023). Antimicrobial PVA hydrogels with tunable mechanical properties and antimicrobial release profiles. *Journal of Functional Biomaterials, 14*, 234.

Guan, Y., Yang, B., Xu, W., Li, D., Wang, S., Ren, Z., Zhang, J., Zhang, T., Liu, X., Li, J., & Li, C. (2022). Cell-derived extracellular matrix materials for tissue engineering. *Tissue Engineering Part B: Reviews, 28*, 1007–1021.

Guo, Z., Liu, H., Shi, Z., Lin, L., Li, Y., Wang, M., & Xue, L. (2022). Responsive hydrogel-based microneedle dressing for diabetic wound healing. *Journal of Materials Chemistry B, 10*, 3501–3511.

Hwang, M. R., Kim, J. O., Lee, J. H., Kim, Y. I., Kim, J. H., Chang, S. W., Jin, S. G., Kim, J. A., Lyoo, W. S., Han, S. S., & Ku, S. K. (2010). Gentamicin-loaded wound dressing with polyvinyl alcohol/dextran hydrogel: Gel characterization and in vivo healing evaluation. *AAPS PharmSciTech, 11*, 1092–1103.

Johnson, K. A., Muzzin, N., Toufanian, S., Slick, R. A., Lawlor, M. W., Seifried, B., & Hoare, T. (2020). Drug-impregnated, pressurized gas-expanded liquid-processed alginate hydrogel scaffolds for accelerated burn wound healing. *Acta Biomaterialia, 112*, 101–111.

Koehler, J., Brandl, F. P., & Goepferich, A. M. (2018). Hydrogel wound dressings for bioactive treatment of acute and chronic wounds. *European Polymer Journal, 100*, 1–11.

Kumar, A., & Kaur, H. (2020). Sprayed in-situ synthesis of polyvinyl alcohol/chitosan loaded silver nanocomposite hydrogel for improved antibacterial effects. *International Journal of Biological Macromolecules, 145*, 950–964.

Lei, J., Chen, P., Li, Y., Wang, X., & Tang, S. (2017). Collagen hydrogel dressing for wound healing and angiogenesis in diabetic rat models. *International Journal of Clinical and Experimental Medicine, 10*, 16319–16327.

Liu, Z., Liu, Z., Shu, B., Lian, C., Wu, J., Wen, Q., & Hu, Y. (2023). One-pot preparation of tough, anti-swelling, antibacterial and conductive multiple-crosslinked hydrogels assisted by phytic acid and ferric trichloride. *Journal of Applied Polymer Science, 140*, e54243.

Luna, L. G. (1968). *Manual of histological staining methods of the Armed Forces Institute of Pathology* (3rd ed.). Blakiston Division, McGraw-Hill.

Martinez-Garcia, F. D., Fischer, T., Hayn, A., Mierke, C. T., Burgess, J. K., & Harmsen, M. C. (2022). A beginner's guide to the characterization of hydrogel microarchitecture for cellular applications. *Gels, 8*, 535.

McInnes, A. D., Moser, M. A., & Chen, X. (2022). Preparation and use of decellularized extracellular matrix for tissue engineering. *Journal of Functional Biomaterials, 13*, 240.

Nath, P. J., Sarma, K. K., & Sarma, B. (2025). Preparation of porcine allogenic acellular diaphragm matrix and its application for umbilical hernioplasty in pig. *Indian Journal of Animal Research, 59*.

Pratheesh, K. V., Nair, R. S., Purnima, C., Raj, R., Mony, M. P., Geetha, C. S., Sobhan, P. K., Ramesan, R. M., Nair, P. D., Thomas, L. V., & Anilkumar, T. V. (2025). An injectable hydrogel of porcine cholecyst extracellular matrix for accelerated wound healing. *Journal of Biomedical Materials Research Part A*.

Rao, T., Phanindra, C. H. V. S., Yamini, M., & Prasad, C. J. I. J. C. P. R. (2021). Hydrogels: The three-dimensional networks—A review. *International Journal of Current Pharmaceutical Research, 13*, 12–17.

Rezvani Ghomi, E., Khalili, S., Nouri Khorasani, S., Esmaeely Neisiany, R., & Ramakrishna, S. (2019). Wound dressings: Current advances and future directions. *Journal of Applied Polymer Science, 136*, 47738.

Rezvani Ghomi, E., Niazi, M., & Ramakrishna, S. (2023). The evolution of wound dressings: From traditional to smart dressings. *Polymer Advances in Technology, 34*, 520–530.

Singh, B., & Kumar, A. (2020). Graft and crosslinked polymerization of polysaccharide gum to form hydrogel wound dressings for drug delivery applications. *Carbohydrate Research, 489*, 107949.

Stubbe, B., Mignon, A., Declercq, H., Van Vlierberghe, S., & Dubruel, P. (2019). Development of gelatin–alginate hydrogels for burn wound treatment. *Macromolecular Bioscience, 19*, 1900123.

Wolf, M. T., Daly, K. A., Brennan-Pierce, E. P., Johnson, S. A., Carruthers, C. A., D'Amore, A., Nagarkar, S. P., Velankar, S. S., & Badylak, S. F. (2012). A hydrogel derived from decellularized dermal extracellular matrix. *Biomaterials, 33*, 7028–7038.

Yang, T. (2012). *Mechanical and swelling properties of hydrogels* (Doctoral dissertation, KTH Royal Institute of Technology).

Yasin, T., Aslam, M. A., Jamil, H., Abdal-Hay, A., Fouad, H., Siddiqi, H. M., & Khan, M. U. A. (2024). Composite hydrogels fabricated from CMC–PVA–GG incorporated with ZIF-8 for wound healing applications. *Journal of Biomaterials Science, Polymer Edition, 35*, 2640–2659.

Yoo, H. J., & Kim, H. D. (2008). Synthesis and properties of waterborne polyurethane hydrogels for wound healing dressings. *Journal of Biomedical Materials Research Part B: Applied Biomaterials, 85*, 326–333.

Yu, T. H., Yeh, T. T., Su, C. Y., Yu, N. Y., Chen, I. C., & Fang, H. W. (2022). Preparation and characterization of extracellular matrix hydrogels derived from acellular cartilage tissue. *Journal of Functional Biomaterials, 13*, 279.

Zhang, W., Liu, Y., Xuan, Y., & Zhang, S. (2022). Synthesis and applications of carboxymethyl cellulose hydrogels. *Gels, 8*, 529. ■